Aluminum Alloy 5083

Subjects: Metallurgy & Metallurgical Engineering
Contributor: Konkrai Nakowong

The semi-solid metal (SSM) 5083 aluminum alloy was developed for part manufacturing in the marine shipbuilding industry and including other industries using this material in the manufacture of parts.

semi-solid metal (SSM) 5083 aluminum alloys | friction stir welding | Taguchi technique | optimized parameter

1. Introduction

Several factors need to be addressed in the manufacture of parts in the marine shipbuilding industry, such as corrosion resistance, strength, and material weight. Aluminum is one of the most popular materials for producing parts because it is lightweight and strong. Aluminum alloy 5083 is one of the materials that meet the criteria because this type of aluminum has a low density, good corrosion resistance, good formability, and is the strongest non-heat-treatable alloy used in annealed conditions [1]. In the manufacture of specific marine ship-building components, a casting process is required. Dendritic microstructures can be formed in most alloy casting processes, which affect the strength of the material. However, improving the structure of the parts through the casting process can be achieved using the semi-solid casting method. This involves forming the metal by casting and partially hardening the metal with nondendritic grains or spheroidal/globular grains. Wannasin J. [2] developed a gas-induced semi-solid process for industrial applications, known as the gas-induced semi-solid (GISS) technique. This process applies fine gas bubble injection, using argon or nitrogen, for example, through a graphite diffuser into metallic water in order to produce semi-solid metals through the principle of metal water displacement and spot heat suction.

Friction stir welding (FSW), a popular marine shipbuilding welding method, involves lower temperatures than the melting temperature. This solid-state welding technique has many advantages, such as producing a fine microstructure, strong welding metallurgical properties, and no loss of mixed elements [3]. Kumar et al. [4] investigated the FSW characteristics in AA5083 and AA6063. The results showed that the welded joints were free from severe defects. The variation in hardness was due to the phase binding of the dissimilar alloys and the changes in the grain structure. Koilraj et al. [5] studied the FSW characteristics of the dissimilar aluminum alloys AA2219 and AA5083 to establish the optimal process parameters using the Taguchi technique. It was found that materials on the advancing side occupied the weld area. The minimum welding hardness occurred in the heat-affected zone (HAZ) on the AA5083 side. Durga Prasad M.V.R et al. [6] optimized the process parameters for FSW on the dissimilar aluminum alloys AA5083 and AA6061 using Taguchi L9 orthogonal array. It was found that the welding speed was an important factor that affected the percentage of elongation and hardness in the weld zone. The tool angle is an important factor in determining the hardness at the HAZ and the thermal–mechanically affected zone (TMAZ). Cavity defects were found in all joints welded with threaded cylindrical tools. Raweni A et al. [7] studied the optimal parameters for FSW on AA5083 using the Taguchi method with a signal-to-noise (S/N) ratio analysis to establish suitable welding parameters and ANOVA to determine the influence between the parameters. Bayazid S.M et al. [8] studied the effects of FSW parameters, such as rotational speed, welding speed, positioning of the joint plate on the microstructure, and mechanical properties of alloys 6063 and 7075 using the Taguchi technique and ANOVA. The results of the study showed that the rotational speed, welding speed, and placement of the plates influenced the tensile strength of the joints by 59%, 30%, and 7%, respectively. A predictive model was established for the tensile strength according to the FSW parameters and the experiments. Shojaeefard M.H et al. [9] studied the mechanical and microstructure properties of AA1100 in FSW using the orthogonal Taguchi L9 experimental design to determine and forecast the optimal grain size value. The ultimate tensile strength and hardness were verified for accuracy by running a confirmation test with the optimal parameters. ANOVA was also performed to determine the most important factor in FSW. Javadi Y et al. [10] studied residual stress arising from the FSW of 5086 aluminum sheets using the Taguchi statistical experimental design to determine the optimal welding parameters, including feed rates, rotational tool, pin speed, pin diameter, and shoulder diameter. The optimal parameters of the process depended on the effect of the residual stress connection parameters. According to ANOVA, it was concluded that the most significant effect on the maximum longitudinal residual stress was the feed rate, whereas the pin and shoulder diameter had no notable effect. The change in rotational speed led to the change in the heat that occurred during welding, which greatly affected the residual stress. Gite R.A et al. [11] criticized the application and parameters of FSW. Sillapasa et al. [12] investigated the fatigue strength of a different friction stir welding process (FSWp) using 6N01 and 7N01 and found it to be adequate. The relationship between the fatigue strength and the hardness was σ_a (R = −1) = 1.68 HV (σ_a is in MPa and HV has no units).

2. Mechanical Property Testing and Metallurgical Structural Inspection

The SSM 5083 aluminum alloy specimens manufactured using the FSW process were prepared for mechanical property testing and analysis of their metallurgical structures, as shown in **Figure 1**.

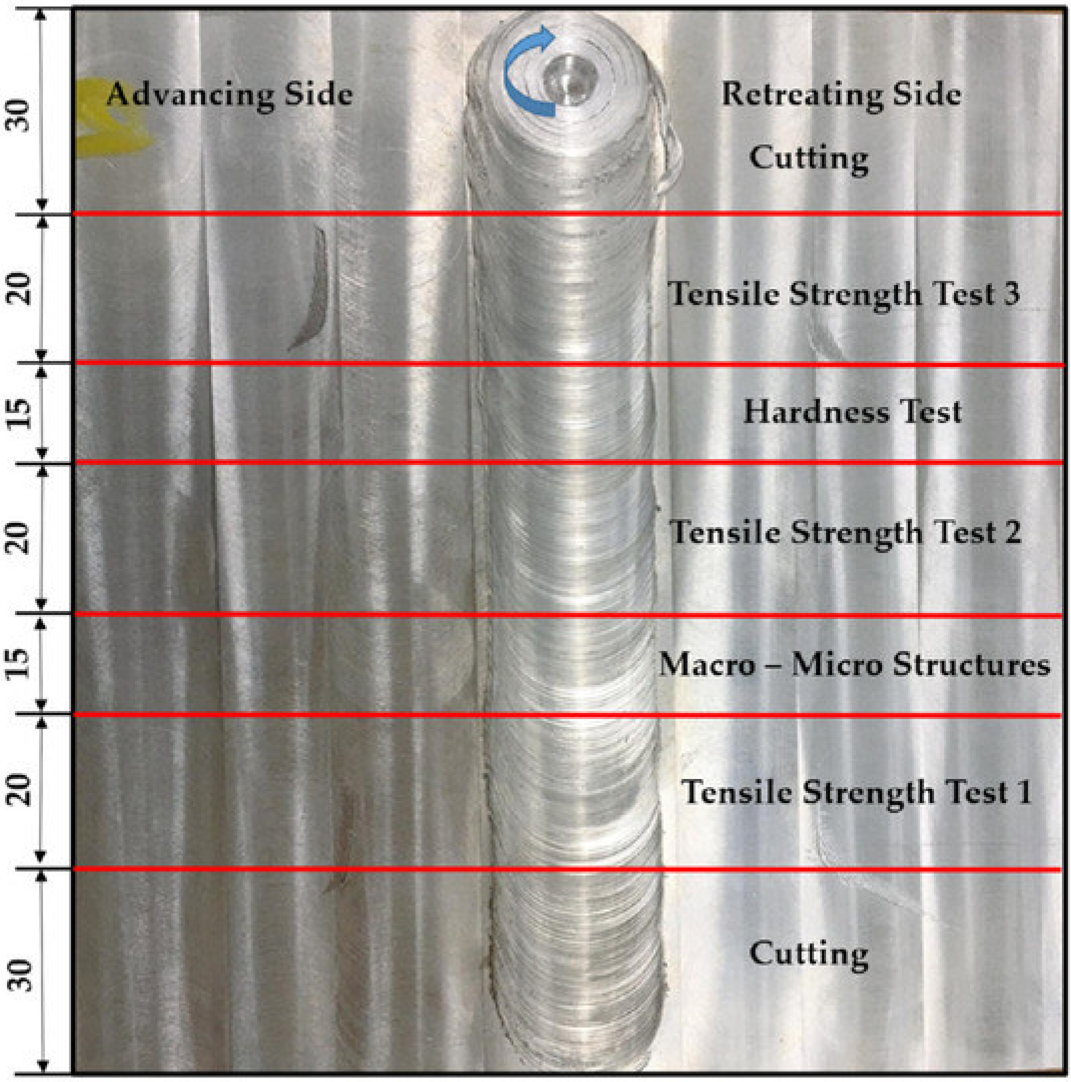

Figure 1. The cutting distance of the welding workpiece for mechanical properties testing and metallurgical structural analysis.

For the preparation of the tensile specimens, a HAAS TM-1 CNC VERTICAL MILLING MACHINE was used to reduce the specimen's width; their thickness and surface features were maintained. The tensile tests were conducted using a universal testing machine (NARIN; model: NRI-CPT500-50 NARIN INSTRUMENT Co., Ltd.; Samut Prakarn, Thailand), according to the American Society for Testing of Materials standard ASTM E8M-04 [13], as shown in **Figure 2**.

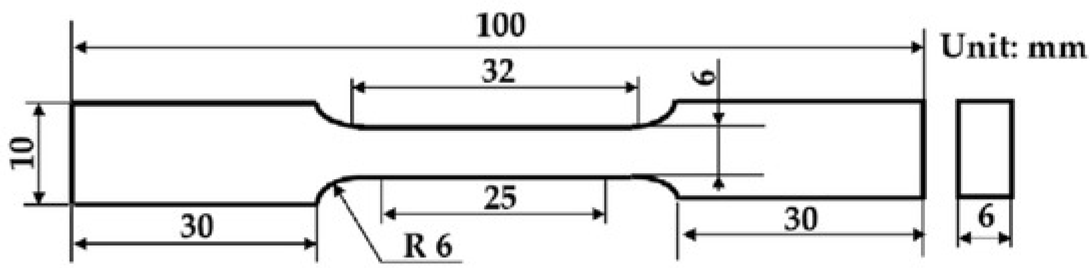

Figure 2. Dimensions of the ASTM E 8M-04 standard tensile specimen [13].

Welding hardness test was performed across the SZ, the HAZ, the TMAZ, and the BM using a Vickers's microhardness tester (SHIMADZU: model: HMV-G Series; Tokyo, Japan) at a load of 0.2 kgf, an indentation distance of 0.2 mm, and an indentation time of 10 s. The distance between the test points was 15 mm from the center of the workpiece on both the advancing side (AS) and the retreating side (RS), as shown in **Figure 3**.

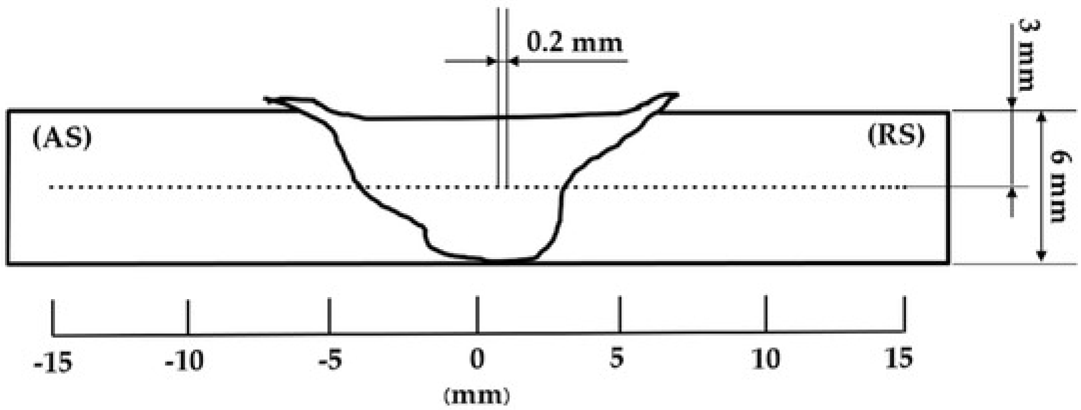

Figure 3. Profile of hardness test positions.

The specimens were prepared for macrostructural analysis using the resin aluminum casting technique. They were then polished using different grades of emery papers: from P220 to P1200. Then, the samples were polished with alumina powder (1–3 microns). Thereafter, the samples were etched with a mixture of 100 mL H_2O and 3 mL HF for 25 s. Finally, they were rinsed with distilled water and wiped clean with alcohol. A hot air gun was used to blow over the samples in order to dry them faster.

The specimens were prepared for microstructural analysis with the same procedure as macrostructural workpieces, except that the samples were etched with the mixture of 190 mL H_2O, 5 mL HNO_3, 3 mL HCl, and 2 mL HF for 10 s. These chemicals were obtained from UBU Materials Laboratory, Ubon Ratchathani University, Ubon Ratchathani, Thailand. An optical electron microscope (LEICA; model: SDM2500M; Wetzlar, Germany) was used to observe the microstructure of the welded joint at the HAZ, the TMAZ, and the SZ. It was equipped with SEM (FEI; model: Quanta 450 FEG; Zurich, Switzerland). EDS (Oxford Instruments; model: X-Max 50; Oxford, UK) was used to analyze the chemical composition.

3. Analysis of Tensile Tests, Vickers Hardness Tests, and Microstructural Examination

From the tensile strength analysis of the rotational speed of 1200 rpm, a welding speed of 10 mm/min, and a threaded cylindrical tool pin profile had the maximum tensile strength at 221 MPa, it was found that the defect location of the specimens occurred at the heat-affected zone on the advancing side (AS-HAZ) because the HAZ had the lowest mechanical properties compared to the other areas. This was because fractures often occurred in the HAZ [14], as shown in Figure 4.

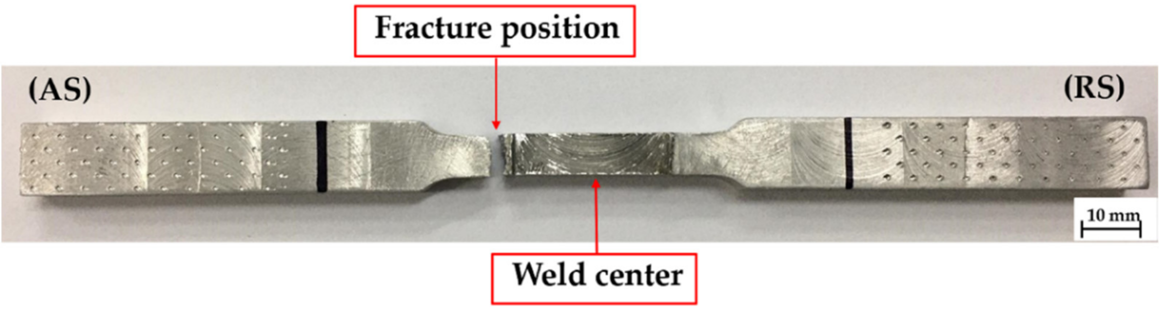

Figure 4. Fracture specimen of tensile test for a rotational speed of 1200 rpm, a welding speed of 10 mm/min, and with a threaded cylindrical tool pin profile.

From the analysis of the hardness in the SZ of the rotational speed of 1200 rpm, a welding speed of 10 mm/min, and a threaded cylindrical tool pin profile had the maximum hardness in the SZ at 81.3 HV, which was in line with the hardness values of the base material at 85 HV, because this type of aluminum cannot improve the thermal-mechanical properties and the hardness mechanism is caused by a solid solution [3]. The lowest hardness value occurred at the AS-HAZ, and nearby, at the thermal–mechanically affected zone on the advancing side (AS-TMAZ), as shown in Figure 5.

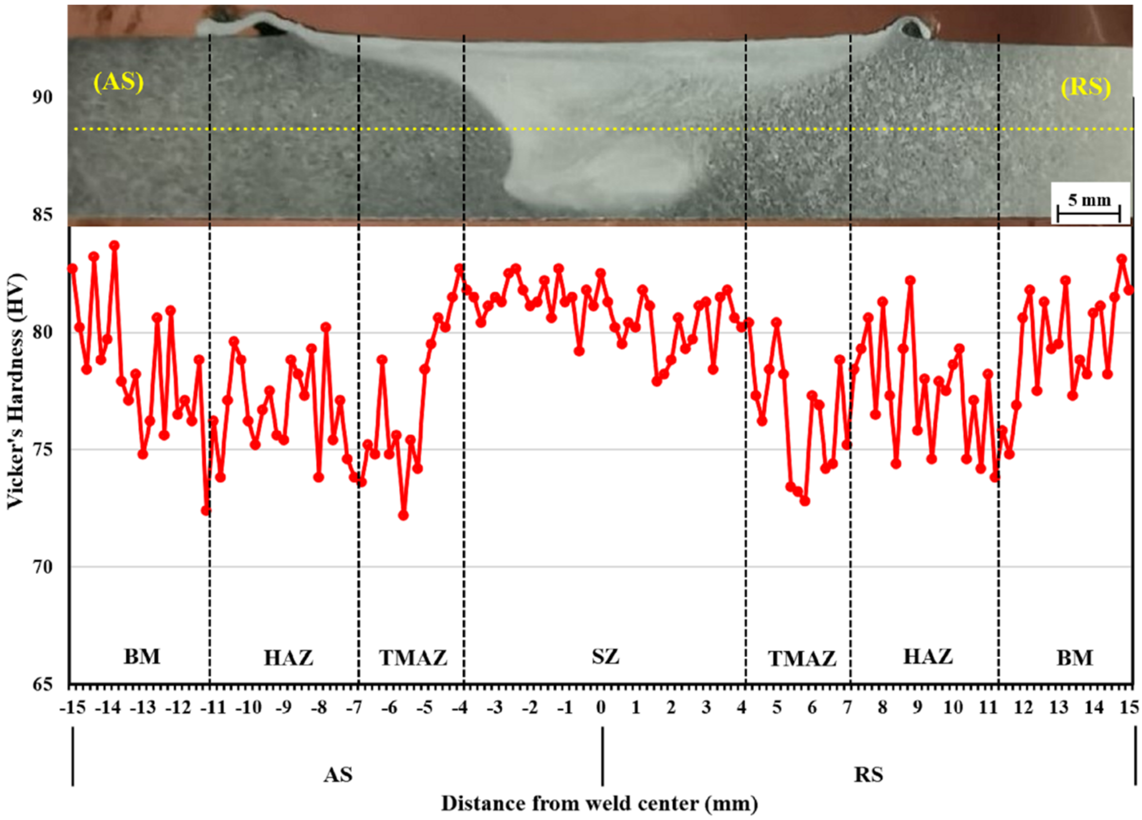

Figure 5. The hardness values at a rotational speed of 1200 rpm, a welding speed of 10 mm/min, and a threaded cylindrical tool pin profile.

The microstructural examination of the welded joint, the joint fabricated with the rotational speed of 1200 rpm, a welding speed of 10 mm/min, and a threaded cylindrical tool pin profile recorded superior hardness in the SZ. Figure 6a shows the AS-TMAZ, in which large grains were formed by the rotation of the pin, causing the flow of metal. The structure in this area was not coordinated; thus, it affected the strength of the
weld joint, which is relevant to the cracking position of the tensile test specimen, as shown in Figure 4. In Figure 6b, fine grains occurred and there was metal flow from both the AS-TMAZ and the thermal–mechanically affected zone on the retreating side (RS-TMAZ), causing appropriate consolidation. However, there were crack defects and irregular consolidation found in the lower central joint due to the lower heat input from the rotating pin. In Figure 6c, there were many void defects in the AS-TMAZ due to the lower heat input from the rotating pin [15][16]. Moreover, as can be seen in Figure 6d, fine grains occurred and there was metal flow in the RS-TMAZ, causing appropriate consolidation.

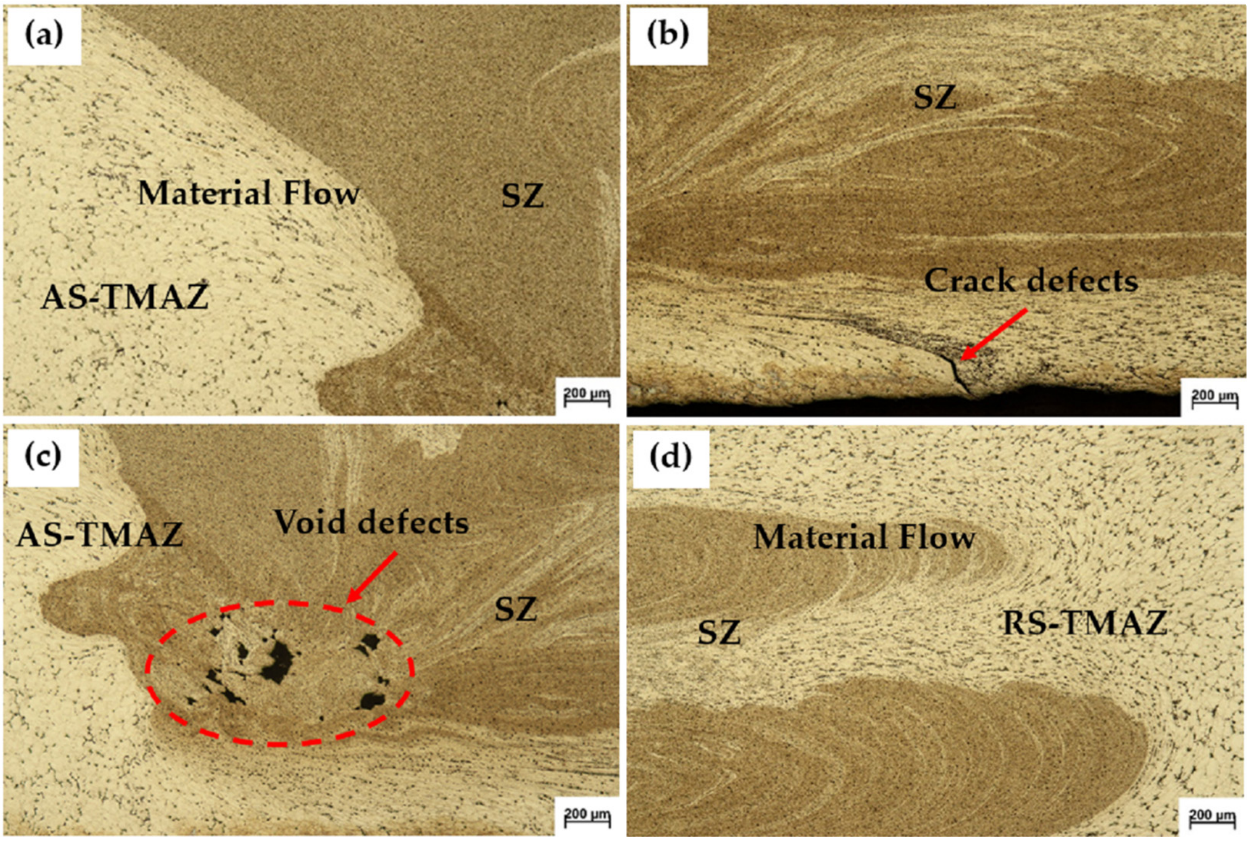

Figure 6. Microstructure of the welded joint at a rotational speed of 1200 rpm, a welding speed of 10 mm/min, and with a threaded cylindrical tool pin profile: (a) AS-TMAZ; (b) SZ; (c) pin tip on the AS; (d) RS-TMAZ.

4. Signal-to-Noise Ratio (S/N Ratio) for the Tensile Strength and the Hardness in the SZ

Signal-to-Noise Ratio (S/N Ratio) The signal-to-noise ratio (S/N ratio) was analyzed for each level of the process parameters, wherein a higher S/N ratio indicates a better weld quality characteristic (the higher, the better) [[17][18]]. Therefore, the optimal process parameter was the one with the highest S/N ratio.

The optimal FSW process parameters for the successful friction stir welding of aluminum alloy SSM 5083 obtained from the tensile strength and the S/N ratio were as follows: A1B1C2: a rotational speed of 1000 rpm, a welding speed of 10 mm/min, and with a threaded cylindrical tool pin profile.

The optimal FSW process parameters for the successful friction stir welding of aluminum alloy SSM 5083 obtained from the hardness in the SZ and the S/N ratio were as follows: A2B1C2: a rotational speed of 1200 rpm, a welding speed of 10 mm/min, and with a threaded cylindrical tool pin profile.

5. Analysis of Variance (ANOVA)

The results were obtained from the ANOVA for the tensile strength and hardness in the SZ. The result proves that the most significant process parameter influencing the tensile strength at a 95% confidence level was welding speed. Contrarily, no parameter (rotational speed, welding speed, or tool pin profile) influenced the hardness in the SZ.

References

1. Nakata, K.; Kim, Y.G.; Ushio, M.; Hashimoto, T.; Jyogan, S. Weldability of high strength aluminum alloys by friction stir welding. ISIJ Int. 2000, 40, 15–19.
2. Wannasin, J.; Janudom, S.; Rattanochaikul, T.; Canyook, R.; Burapa, R.; Chucheep, T.; Thanabumrungkul, S. Research and development of gas induced semi-solid process for industrial applications. Trans. Nonferrous Met. Soc. China 2010, 20, 1010–1015.
3. Mishra, R.S.; Ma, Z.Y. Friction stir welding and processing. Mater. Sci. Eng. 2005, 50, 1–78.
4. Kumar, S.; Srivastava, A.K.; Singh, R.K.; Dwivedi, S.P. Experimental study on hardness and fatigue behavior in joining of AA5083 and AA6063 by friction stir welding. Mater. Today Proc. 2020, 25, 646–648.
5. Koilraj, M.; Sundareswaran, V.; Vijayan, S.; Koteswara Rao, S.R. Friction stir welding of dissimilar aluminum alloys AA2219 to AA5083 Optimization of process parameters using Taguchi technique. Mater. Des. 2012, 42, 1–7.
6. Durga Prasad, M.V.R.; Namala, K.K. Process Parameters Optimization in Friction Stir Welding by ANOVA. Mater. Today Proc. 2018, 5, 4824–4831.

7. Raweni, A.; Majstorovic, V.; Sedmak, A.; Tadic, S.; Kirin, S. Optimization of AA5083 Friction Stir Welding Parameters Using Taguchi Method. Teh. Vjesn. Tech. Gaz. 2018, 25, 861–866.
8. Bayazid, S.M.; Farhangia, H.; Ghahramania, A. Investigation of friction stir welding parameters of 6063-7075 Aluminum alloys by Taguchi method. Procedia Mater. Sci. 2015, 11, 6–11.
9. Shojaeefard, M.H.; Akbari, M.; Khalkhali, A.; Asadi, P.; Parivar, A.H. Optimization of microstructural and mechanical properties of friction stir welding using the cellular automaton and Taguchi method. Mater. Des. 2014, 64, 660–666.
10. Javadi, Y.; Sadeghi, S.; Najafabadi, M.A. Taguchi optimization and ultrasonic measurement of residual stresses in the friction stir welding. Mater. Des. 2014, 55, 27–34.
11. Gite, R.A.; Loharkar, P.K.; Shimpi, R. Friction stir welding parameters and application: A review. Mater. Today Proc. 2019, 19, 361–365.
12. Sillapasa, K.; Mutoh, Y.; Miyashita, Y.; Seo, N. Fatigue Strength Estimation Based on Local Mechanical Properties for Aluminum Alloy FSW Joints. Materials 2017, 10, 186.
13. ASTM International. Standard Test Methods for Tension Testing of Metallic Materials E 8M—04. In Annual Book of ASTM Standard; ASTM International: West Conshohocken, PA, USA, 1996; Volume 03.01, pp. 1–24.
14. Shahraki, S.; Khorasani, S.; Behnagh, R.A.; Fotouhi, Y.; Bisadi, H. Producing of AA5083/ZrO2 nanocomposite by friction stir processing (FSP). Metall. Mater. Trans. B 2013, 44, 1546–1553.
15. Cho, J.-H.; Boyce, D.E.; Dawson, P.R. Modeling strain hardening and texture evolution in friction stir welding of stainless steel. Mater. Sci. Eng. A 2005, 398, 146–163.
16. Nandan, R.; DebRoy, T.; Bhadeshia, H.K.D.H. Recent advances in friction-stir welding-process-weldment structure and properties. Prog. Mater Sci. 2008, 53, 980–1023.
17. Vijayan, S.; Raju, R.; Subbaiah, K.; Sridhar, N.; Rao, S.R.K. Friction stir welding of Al–Mg alloy-optimization of process parameters using Taguchi method. Exp. Tech. 2010, 34, 37–44.
18. D’Urso, G.; Giardini, C. The influence of process parameters and tool geometry on mechanical properties of friction stir welded aluminum lap joints. Int. J. Mater. Form. 2010, 3, 1011–1014.